How to Cite: Kholturaev, B.Zh., Yunusov, K.E., Yuldoshov, S.A., Sarymsakov, A.A., Atakhanov, A.A., Xakimov, Z.Z., Abdalkarim, S.Y.H., Yu, H., Jiang, G., & Niu, L.N. (2026) Stepwise Chemical Oxidation of Cellulose to Tricarboxycellulose: Synthesis, Structural Characterization, and Hemostatic Properties. *Eurasian Journal of Chemistry*. https://doi.org/10.31489/2959-0663/4-26-3

Article

Received: 22 August 2026 | Revised: 3 November 2026 |
Accepted: 4 November 2026 | Published online: 11 November 2026

UDC 547.458.83

https://doi.org/10.31489/2959-0663/4-26-3

Bakhriddin Zh. Kholturaev[1], Khaydar E. Yunusov[1]*, Sherzod A. Yuldoshov[1], Abdushkur A. Sarymsakov[1], Abdumutolib A. Atakhanov[1], Ziyoviddin Z. Xakimov[2], Somia Yassin Hussain Abdalkarim[3], Houyong Yu[3], Guohua Jiang[3], Li-Na Niu[4]

[1]*Institute of Polymer Chemistry and Physics, Academy of Sciences of the Republic of Uzbekistan, Tashkent, Uzbekistan*
[2]*Tashkent Medical Academy, Tashkent, Uzbekistan*
[3]*School of Materials Science and Engineering, Zhejiang Sci–Tech University, Hangzhou, China*
[4]*School of Stomatology, The Fourth Military Medical University, Xi'an, Shaanxi, China*
*(*Corresponding author's e-mail: silver4727@yahoo.com)*

Stepwise Chemical Oxidation of Cellulose to Tricarboxycellulose: Synthesis, Structural Characterization, and Hemostatic Properties

Highly oxidized cellulose materials were prepared from cotton cellulose (CC), woven gauze (WG), and medical cotton (MC) through sequential treatment with sodium hypochlorite (NaClO), sodium periodate ($NaIO_4$), and hydrogen peroxide (H_2O_2), with the aim of introducing additional carboxyl functional groups. The structural evolution of cellulose during each oxidation step was investigated by Fourier-transform infrared (FT-IR) spectroscopy, which confirmed the formation of aldehyde, carboxyl, and carboxylate groups while preserving the β-1,4-glycosidic backbone. Quantitative analysis revealed that the final tricarboxycellulose samples contained up to 11.95±0.12 mmol/g, 10.55±0.11 mmol/g, and 9.40±0.10 mmol/g carboxyl groups for CC-, WG-, and MC-derived materials, respectively. The introduction of multiple hydrophilic functionalities significantly improved water absorption and swelling behavior. The highest swelling degree was observed for tricarboxycellulose derived from cotton cellulose, reaching 830±16.6% after 20 min, whereas samples prepared from woven gauze and medical cotton exhibited maximum swelling values of 670±13.4% and 530±10.6%, respectively. The enhanced swelling capacity was attributed to increased hydrophilicity, disruption of crystalline regions, and the formation of a more open and porous polymer network. Tricarboxycellulose prepared from cotton cellulose exhibited the most effective hemostatic activity, with a bleeding time of 69±3.24 sec and a blood clotting index of 55.6±0.15%, outperforming commercial oxidized cellulose powder.

Keywords: cotton cellulose, woven gauze, medical cotton, tricarboxycellulose, cellulose oxidation, dialdehyde cellulose, carboxyl groups, swelling behavior, hemostatic properties

Introduction

Cellulose has emerged as a promising sustainable biopolymer because of its renewable origin, biodegradability, biocompatibility, low toxicity, and suitable mechanical characteristics, which enable its use as an eco-friendly substitute for synthetic materials in various applications [1]. Although cellulose possesses several attractive properties, its dissolution remains difficult in water and most conventional organic solvents because of the compact crystalline arrangement of its chains and the strong hydrogen-bonding interactions formed within and between the polymer chains [2, 3]. The insolubility of cellulose is attributed to its chemical structure and several related structural factors. In particular, cellulose is a high degree of polymerization macromolecule whose dissolution is restricted by strong intra- and intermolecular hydrogen-bonding interactions and by the reduced entropic driving force associated with dissolving long polymer chains [4, 5]. Secondly, each anhydroglucose unit of cellulose contains three hydroxyl groups together with ring and glycosidic oxygen atoms, which participate in extensive intra- and intermolecular hydrogen-bonding interactions [6]. The hydroxyl groups located at the C2, C3, and C6 positions of cellulose act as the main reactive sites for chemical modification, allowing the production of various cellulose derivatives with tailored properties [7].

Oxidation of cellulose using different oxidizing systems can generate oxidized cellulose derivatives containing various functional groups, including aldehyde, ketone, and carboxyl groups [8, 9].

© 2026 The Authors. This is an open access article under the CC BY-NC-ND license (http://creativecommons.org/licenses/by-nc-nd/4.0/)

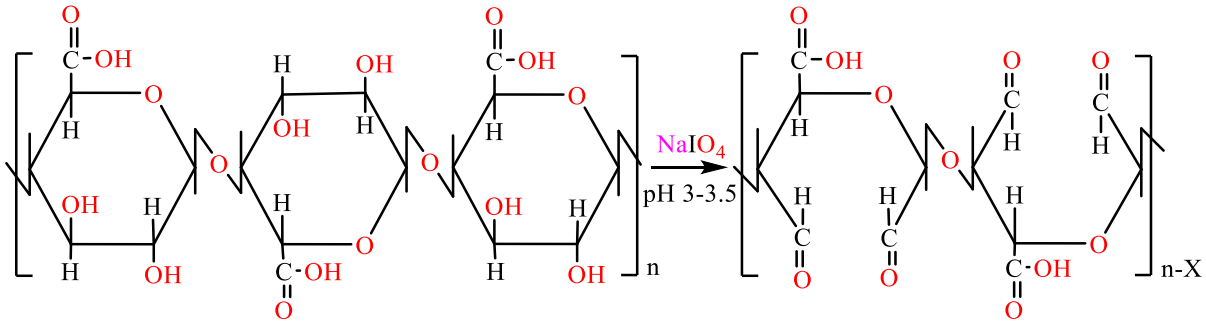
Oxidation of cellulose can be performed using different oxidizing systems, including nitrogen oxide, nitric acid based oxidants, sodium chlorite, peroxides, periodate, and other selective oxidation systems [10-12].

The selectivity and efficiency of cellulose oxidation are strongly influenced by the oxidizing system, reaction pH, temperature, solvent environment, and other process parameters [12, 13]. The structure of oxidized cellulose derivatives depends strongly on the oxidation system, as different oxidants introduce functional groups at distinct positions of the anhydroglucose unit, such as C6 carboxylation via TEMPO oxidation and C2, C3 carboxylation via periodate-chlorite oxidation [14].

The oxidation pathway of cellulose depends on the position of the hydroxyl groups: primary hydroxyl groups at the C6 position can be converted into aldehyde or carboxylic acid groups, whereas oxidation of secondary hydroxyl groups at C2 and C3 commonly leads to the formation of dialdehyde structures through periodate-mediated C2-C3 bond cleavage [15, 16]. Periodate oxidation selectively cleaves the C2–C3 vicinal diol units of cellulose, leading to pyranose ring opening and the formation of dialdehyde cellulose, while subsequent chlorite oxidation converts the aldehyde groups into dicarboxylated cellulose structures [17].

The oxidizing agents most widely used in the selective oxidation of cellulose include nitroxyl radicals and sodium periodate [13, 18]. Sodium periodate is an effective reagent for the selective oxidation of cellulose because it targets the vicinal diol groups at the C2 and C3 positions of the anhydroglucose unit, resulting in C2–C3 bond cleavage and the formation of dialdehyde cellulose structures [19]. Sodium periodate ($NaIO_4$) oxidation of cellulose leads to the formation of dialdehyde cellulose (DAC) through selective cleavage of C2–C3 vicinal diol groups [20].

Periodate oxidation of cellulose is commonly conducted in aqueous media under mild conditions, typically at 25 ℃ temperatures, to produce dialdehyde cellulose structures [21]. Under these conditions, the mechanism of selective oxidation of cellulose in the presence of sodium periodate under mild conditions is shown in Scheme 1.



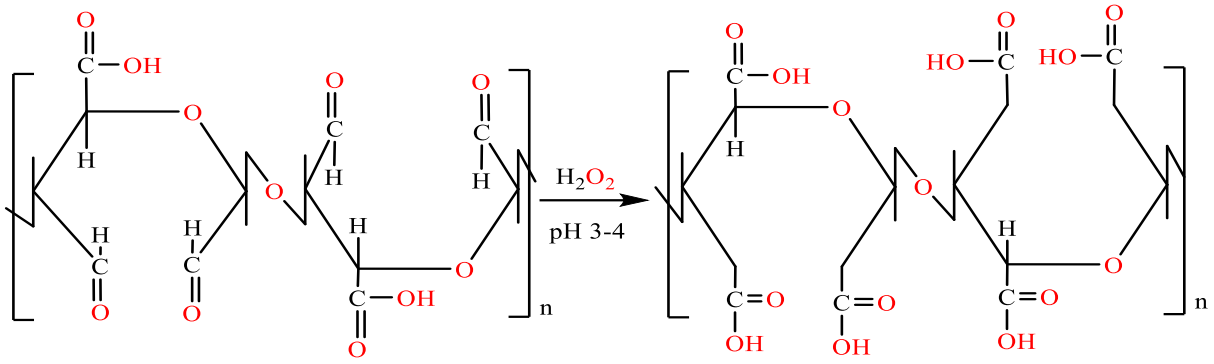
Scheme 1. Selective oxidation of cellulose using sodium periodate [22].

One of the advantages of this method is its high yield and the ability to readily produce dispersible cellulose nanofibrils (Scheme 1). Moreover, the aldehyde groups obtained during oxidation may undergo further conversion into carboxylic acids or react with amines to produce Schiff bases [23-25]. At the initial stage of the reaction, periodate ions attack the C2-C3 bonds in the crystalline regions, resulting in disruption of the highly ordered macromolecular structure [26]. Periodate oxidation introduced reactive aldehyde groups that formed hemiacetal and hemialdal linkages during film formation, contributing to improved mechanical performance and water barrier properties [27].

In order to reduce the reaction time, the oxidation was carried out at temperatures above 85 °C using metal salts (LiCl, $ZnCl_2$, $CaCl_2$) as cellulose activators, despite the fact that periodate decomposes at temperatures above 55 °C [28]. It has been demonstrated that, under such conditions, dialdehyde cellulose (DAC) containing a high amount of aldehyde groups may be produced at comparatively low periodate concentrations [29].

Hydrogen peroxide treatment under mildly acidic conditions induces oxidative modifications in wood-derived cellulose fibers, resulting in an increased content of carbonyl-containing functional groups [30]. It has been demonstrated that the use of widely employed oxidants, including H_2O_2, enables the introduction of carbonyl groups into the cellulose structure [31]. Furthermore, it has been noted that the large-scale production of cellulose with enhanced moisture resistance can be achieved even without the use of additional

additives [32]. The behavior and reaction mechanism of H_2O_2 at alkaline pH have been successfully investigated, as shown in Scheme 2.



Scheme 2. Mechanism of H_2O_2-mediated oxidation of aldehyde groups to carboxyl groups.

During the oxidation process under alkaline pH conditions, the main effect is attributed to the hydroperoxide anion generated from the decomposition of hydrogen peroxide, resulting in a pH medium range of 10-12. At low pH values, hydrogen peroxide undergoes decomposition either via the Fenton reaction [33] with metals or through interaction with organic substances, such as cellulose, leading to the formation of hydroxyl radicals [34]. Hydroxyl radicals can react with several atoms of the carbohydrate chains, with the primary sites being the oxidation of secondary hydroxyl groups or the anomeric carbon atom. The oxidation process is initiated by the abstraction of a hydrogen radical from the carbon atom associated with a secondary hydroxyl group, ultimately leading to the incorporation of oxygen and the formation of a ketone functional group [35].

Acidic ozonation can promote radical-mediated oxidation of cellulose, resulting in the formation of carbonyl groups and partial cleavage of the polymer chains. Hydroxyl-radical attack near the anomeric C1 position may contribute to hydrogen abstraction, chain scission, and the development of oxidized carbonyl-containing structures [36].

H_2O_2-based oxidation is considered a relatively environmentally benign process because hydrogen peroxide decomposes into water and oxygen, minimizing persistent chemical residues [37]. Hydrogen peroxide is considered an environmentally benign oxidant because its decomposition mainly produces water and oxygen; however, under certain reaction conditions, reactive oxygen species generated from H_2O_2 can promote cellulose degradation and side reactions [38].

The development of highly functionalized cellulose derivatives requires oxidation strategies capable of modifying different reactive sites within the anhydroglucose units while maintaining an appropriate balance between functional-group density and structural integrity. The introduction of oxygen-containing functionalities, particularly carboxyl groups, is of considerable interest for biomedical applications because it can influence cellulose hydration, swelling behavior, and interactions with blood components [39].

Conventional TEMPO-mediated oxidation provides an efficient and regioselective pathway for converting primary hydroxyl groups at the C6 position into carboxyl functionalities, whereas direct functionalization of the secondary C2 and C3 positions remains limited under typical reaction conditions [40]. Enzymatic oxidation represents another promising approach; however, its regioselectivity is governed by the catalytic characteristics of the enzymes employed, with lytic polysaccharide monooxygenases predominantly targeting positions associated with oxidative cleavage of glycosidic linkages [41]. In contrast, periodate oxidation provides access to the C2-C3 positions through selective cleavage of vicinal diol groups, generating reactive dialdehyde structures [42]. These aldehyde functionalities can subsequently undergo further oxidation to carboxyl groups. Previous investigations have demonstrated the feasibility of combining periodate oxidation with hydrogen peroxide treatment to increase the carboxyl functionalization of cellulosic materials [43]. Nevertheless, extensive oxidation may also promote polymer-chain degradation, highlighting the importance of controlling the reaction conditions [44].

Based on these considerations, the present study investigates a sequential NaClO-$NaIO_4$-H_2O_2 oxidation strategy designed to integrate three complementary chemical transformations: initial oxidation of accessible hydroxyl groups, selective generation of C2-C3 dialdehyde functionalities, and subsequent

oxidation of carbonyl-containing intermediates toward additional carboxyl groups. The final H_2O_2 treatment is introduced specifically to promote the conversion of periodate-generated aldehyde functionalities, thereby providing a distinct chemical purpose for the third stage. Rather than seeking procedural simplicity, this approach aims to extend cellulose functionalization beyond the predominantly C6-selective pathways and obtain highly carboxylated materials with tailored physicochemical properties.

This study aims to characterize highly oxidized cellulose obtained from cotton cellulose, woven gauze, and medical cotton and to determine how the oxidation process influences carboxyl-group content, swelling capacity, and hemostatic performance.

Experimental

Materials

Cotton cellulose (CC, $(C_6H_{10}O_5)_n$, ≥98%, degree crystalline (DC)=84, degree polymerization (DP)=1200) was purchased from Promxim Impex Ltd. (Uzbekistan); woven gauze (WG), medical cotton bandage, (CC≤95%, DC=65, DP=970) was obtained from Jizzakh Chemical Plant LLC (Uzbekistan); and medical cotton (MC) (CC≤98% DC=70, DP=1050) was purchased from Midicot Ltd. (Uzbekistan). Sodium hypochlorite (NaClO, 10-15%, CAS No. 7681-52-9), sodium periodate ($NaIO_4$, ≥99%, CAS No. 7790-28-5), hydrogen peroxide (H_2O_2, 30-35%, CAS No. 7722-84-1), hydrochloric acid (HCl, CAS No. 7647-01-0), sulfuric acid (H_2SO_4, 96-98%, CAS No. 7664-93-9), hydroxylamine (NH_2OH, 50 wt.% in H_2O, CAS No. 7803-49-8), and sodium hydroxide (NaOH, 98.0%, CAS No. 1310-73-2) were purchased from Sigma-Aldrich. Commercial SURGICEL® Powder Absorbable Hemostat (oxidized regenerated cellulose (ORC), Ethicon, LLC, San Lorenzo, Puerto Rico, USA), containing 3 g of ORC powder, was used as a reference hemostatic material. Distilled water (CAS No. 7732-18-5) was used throughout the experiments. All other chemicals were of analytical grade.

Method for the Preparation of Tricarboxycellulose

The oxidation reaction was carried out through the stepwise oxidation of cellulose for its application as a hemostatic agent. In the first stage, 5 g of cellulose was treated with a 14 g/l NaClO solution at a 1:10 volume ratio for 3-4 hours at 60 ℃. After the process, the oxidized cellulose was filtered, washed 4-6 times with distilled water until neutral pH was achieved, and lyophilized for 10-12 hours at 80 °C. To increase the carboxyl group content in the oxidized cellulose obtained using NaClO solution, sodium periodate ($NaIO_4$) was used to cleave the C2-C3 carbon bond. In the subsequent step, the reaction was carried out using a 1.5-2.5% $NaIO_4$ solution for 10-15 minutes at 30-35 °C. The oxidized cellulose sample was washed 10-12 times with distilled water until a neutral medium was achieved and then lyophilized for 6-8 hours at 80 °C. In the final stage, 3 g of oxidized cellulose was treated with 4-10% H_2O_2 at a 1:10 mass ratio for 1-3 hours at 70-80 °C. The resulting reaction mixture was filtered, washed until a neutral medium was achieved, and dried to a moisture content of 4 ± 0.5% [45].

Determination of the Swelling Degree of Tricarboxycellulose

The water retention value (WRV) method [46] is considered one of the most effective approaches for evaluating the swelling capacity of oxidized cellulose. Initially, 0.2000-0.5000 g of dry tricarboxycellulose was accurately weighed, and the sample was allowed to swell in distilled water for 30 minutes at 25-30 °C.

Subsequently, the sample was filtered through membranes with a pore size of 50-200 nm, and excess water was removed using dry filter paper. The sample was then centrifuged at 8000 rpm for 10 minutes, after which the wet weight was determined.

The following formula was used to calculate the swelling degree of tricarboxycellulose:

$$WRV\ (g/g) = (m_2 - m_1) / m_1, \quad (1)$$

where: m_1 - is the initial dry mass of tricarboxycellulose *(g)*; m_2 - is the mass of tricarboxycellulose *(g)*, filtered and dried to constant weight.

Infrared Spectroscopic Analysis Method

The structure of the samples was analyzed using an “Inventio-S” FT-IR spectrophotometer (Bruker, Germany) in the wavelength range of 500-4000 cm^{-1}.

Determination of Carboxyl Groups

The content of carboxyl groups (mmol/g) in tricarboxycellulose samples was determined by titration using a Mettler Toledo conductometer (Mettler Toledo, Switzerland). In this procedure, 0.2 g of tricarboxycellulose was added to 20 ml of 0.1 N HCl solution and stirred for 15 minutes, after which the resulting suspension was titrated with 0.5 N NaOH [47]. The content of carboxyl groups in the tricarboxycellulose sample was determined using the following formula:

$$\text{Carboxyl content (mmol/g)} = V \times N / W \times 1000, \quad (2)$$

where: *V* – is the volume of NaOH consumed (ml); *N* – is the normality of NaOH (typically 0.1); *W* – is the mass of the sample (g).

Determination of the pH Value

The pH values were determined using a FiveEasy Plus FP20 pH/mV meter (Mettler Toledo, Switzerland), which measures the proton (H^+) concentration in the solution.

Determination of the Aldehyde Group Content in DAC

In 25 ml distilled water, 0.5 g of DAC were dispersed. Then, 25 ml of 0.25 M hydroxylamine hydrochloride solution was added, and the pH was adjusted to approximately 4.0 using 0.1 M HCl solution and stirred at 25 °C for 4 hours to ensure complete reaction between aldehyde groups and hydroxylamine hydrochloride. After completion of the reaction, the released hydrochloric acid was titrated with standardized 0.1 M NaOH solution until the endpoint (pH 4.0-4.5 or phenolphthalein indicator endpoint) was reached. A blank experiment was carried out under the same conditions without the sample. The number of aldehyde groups in the DAC was calculated using the following equation:

$$(\text{AG})\text{Aldehyde content}(\text{mmol/g}) = \frac{(V_1 - V_0) \times C_M}{m}, \quad (3)$$

where: *AG* – is the aldehyde group content, (mmol/g); C_M – is the molar concentration of the consumed NaOH, mol/l; *Va* – is the volume of alkali consumed for DAC, *(ml)*; *m* – is the mass of the dry sample, *(g)*; *Vb* – is the volume of alkali consumed for cellulose, *(ml)*; *Mr* – is the molecular weight of dialdehyde cellulose, *(g/mol)*.

Determination of Hemostatic Properties

The hemostatic properties of oxidized cellulose were evaluated using the whole blood clotting assay. Fresh animal blood anticoagulated with sodium citrate was used for the experiment. A known amount of oxidized cellulose sample was placed in a test tube, and a fixed volume of blood was added onto the material surface. Subsequently, $CaCl_2$ solution was introduced to initiate coagulation, and the mixture was incubated at 37 °C for a predetermined time interval.

After incubation, distilled water was added carefully to lyse the non-coagulated red blood cells. The obtained suspension was analyzed spectrophotometrically by measuring the absorbance of hemoglobin at 540 nm. Lower absorbance values indicated better blood clotting ability and higher hemostatic activity of the oxidized cellulose samples. A blank experiment without the sample was performed under identical conditions for comparison.

The blood clotting index (BCI) was calculated according to the following equation:

$$\text{BCI (\%)} = A_s/A_c \times 100, \quad (4)$$

where: A_s - is the absorbance of the sample; A_c - is the absorbance of the control sample. Lower BCI values correspond to improved hemostatic performance.

Hemostatic Evaluation Using Hemorrhage Models

The hemostatic performance of the powdered agent was assessed using a standardized rat liver injury model. Under general anesthesia, laparotomy was performed to expose the liver, and the right liver lobe was selected as the bleeding site. A uniform parenchymal injury of 5×5 mm in area and approximately 2 mm in depth was created. Immediately after wound formation, 0.05-0.10 g of the powdered hemostatic material was applied to the injury surface. Hemostatic efficacy was evaluated based main parameters of time to

hemostasis. The time to hemostasis was measured with a stopwatch from the onset of bleeding until complete bleeding cessation [46].

Statistical Analysis

The data were recorded and analyzed using Origin 8.5 software. The results are reported as the means ± standard deviation (SD). ANOVA software was used to evaluate statistically significant differences between multiple groups, with a P-value of less than 0.05 considered significant and a P-value of less than 0.01 considered highly substantial.

Results and Discussion

To establish the reaction conditions for oxidized cellulose production, cotton cellulose (CC), woven gauze (WG), and medical cotton (MC) were selected as initial materials and oxidized using sodium hypochlorite (NaClO) solution. The influence of reaction parameters on the oxidation efficiency and properties of the obtained oxidized cellulose was systematically investigated. In this process, the effects of various factors on oxidation, including oxidant concentration, reaction duration, and temperature, were investigated. Under various conditions, the content of carboxyl groups in the samples and the product yields were determined, and results are presented in Table 1.

Table 1

Oxidation of CC, WG, and MC using sodium hypochlorite (NaClO) solution

Samples	C(NaClO), g/L	pH	Reaction duration, h	T, °C	Content of carboxyl groups (-COOH), mmol/g	Yield, %
CC	14	9-9.5	3	40	1.33±0.019	68±2.72
			4	40	1.67±0.025	64±2.56
			3	50	1.87±0.028	58±2.32
			4	50	2.00±0.030	53±2.12
			3	60	2.33±0.035	48±1.92
			4	**60**	**3.11±0.046**	**44±1.76**
WG	14	9-9.5	3	40	1.16±0.017	65±2.61
			4	40	1.44±0.021	59±2.36
			3	50	1.51±0.022	55±2.21
			4	50	1.78±0.026	50±2.01
			3	60	1.82±0.027	45±1.81
			4	**60**	**2.40±0.036**	**40±1.61**
MC	14	9-9.5	3	40	1.00±0.001	78±3.12
			4	40	1.29±0.019	70±2.81
			3	50	1.47±0.022	66±2.64
			4	50	1.60±0.024	60±2.41
			3	60	1.73±0.026	56±2.24
			4	**60**	**2.11±0.031**	**50±2.05**

As shown in Table 1, the application of a 14 g/L NaClO solution markedly promotes cellulose oxidation by converting primary hydroxyl groups into carboxyl groups, thereby enhancing the efficiency of the modification process. During the oxidation process, the reaction efficiency is significantly dependent on the pH of the medium. The reaction conditions were achieved at pH 9.0-9.5, where NaClO remained sufficiently stable and reactive. At pH values below 7, rapid decomposition of NaClO reduced the availability of active oxidizing species. Conversely, strongly alkaline conditions above pH 11 induced cellulose degradation, adversely affecting the structural integrity of the oxidized samples.

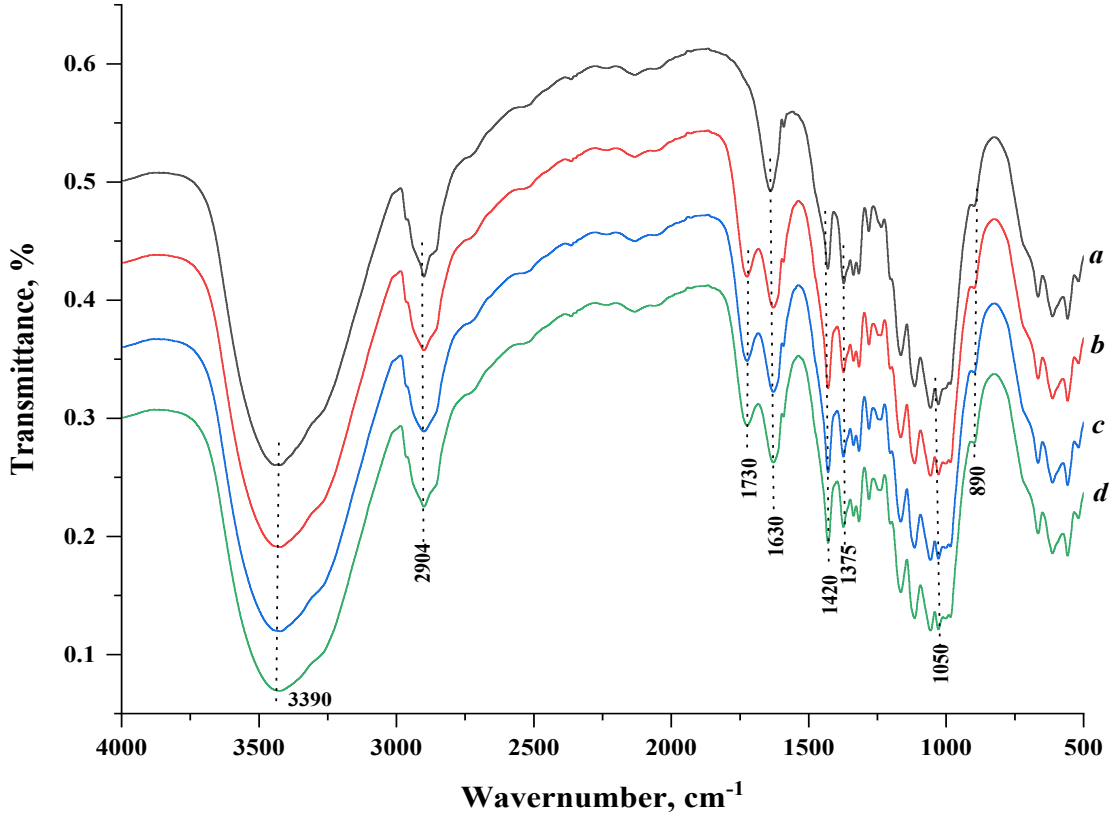
The reaction duration directly affects the carboxyl group content and the product yield. The reduced yield may result from cellulose depolymerization and the formation of water-soluble sodium carboxylates, which are partially lost during product isolation.

The experimental results revealed that the oxidation time is a critical parameter controlling both the degree of functionalization and the preservation of cellulose integrity. A reaction period of 2-3 h was not sufficient for effective carboxyl group formation. However, prolonged oxidation for 5-6 h led to excessive

interaction with the oxidizing agent, resulting in partial degradation of cellulose molecules. Thus, the 4 h reaction time was identified as the reaction conditions, yielding the highest-quality product (Table 1).

Overall, prolongation of the reaction time significantly enhanced cellulose oxidation, as evidenced by the increased carboxyl group contents of 3.11±0.046 mmol/g, 2.40±0.036 mmol/g, and 2.11±0.031 mmol/g for CC, WG, and MC, respectively. However, the higher degree of oxidation was accompanied by a substantial reduction in product yield, reflecting partial degradation of the cellulose matrix and resulting in yields of 44±1.76%, 40±1.61%, and 50±2.05%, respectively.

The FT-IR spectra of oxidized CC, WG, and MC prepared by NaClO-mediated oxidation are shown in Figure 1.



a. Cellulose; **b.** OC obtained by oxidizing CC; **c.** OC obtained by oxidizing WG; **d.** OC obtained by oxidizing MC.
Figure 1. FT-IR spectroscopic results of mono-carboxylated cellulose samples.

The FT-IR spectra presented in Figure 1 reveal notable structural modifications in CC, WG, and MC after NaClO oxidation, as evidenced by the emergence and intensification of absorption bands corresponding to carbonyl and carboxyl groups.

A characteristic broad absorption band observed at 3340-3400 cm^{-1} in the spectrum of native cotton cellulose corresponds to the O-H stretching vibrations of hydroxyl groups involved in intra- and intermolecular hydrogen bonding. After NaClO-mediated oxidation, the diminished intensity and reduced width of this band indicate the partial oxidation of hydroxyl groups to carbonyl and carboxyl groups, resulting in decreased hydrogen-bonding interactions within the cellulose matrix. This transformation also reflects partial disruption of crystalline regions and the formation of amorphous domains within the cellulose matrix.

The absorption peak located in the 2890-2925 cm^{-1} region corresponds to the C-H stretching vibrations of aliphatic CH and CH_2 groups. Its relatively unchanged appearance across all samples indicates that NaClO oxidation predominantly occurred at hydroxyl functionalities without causing significant alterations to the cellulose backbone.

The appearance of new absorption bands at 1720-1740 cm^{-1} in the oxidized samples confirms the successful oxidation of cellulose, as these bands are associated with the C=O stretching vibrations of newly formed carboxyl and aldehyde groups. These peaks are weak in the unmodified cellulose but become prominent in the oxidized samples, confirming the successful introduction of carbonyl functionalities. Among the

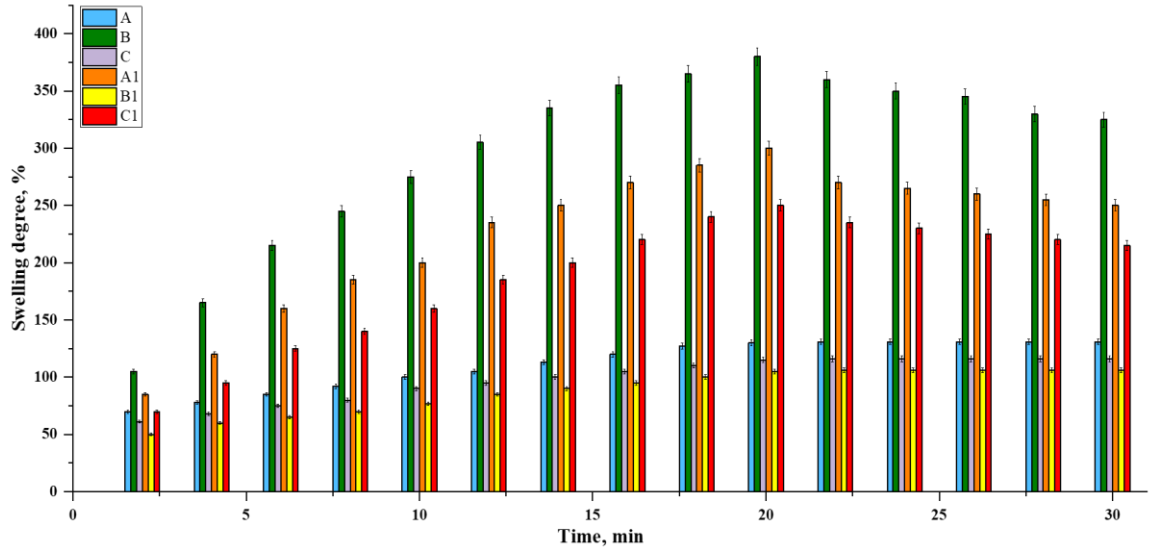
three oxidized samples, the intensity of this band follows the order CC > WG > MC, which correlates with the quantitative increase in carboxyl group content 3.11±0.046 mmol/g, 2.40±0.036 mmol/g, and 2.11±0.031 mmol/g, respectively. The higher reactivity of pure cellulose is attributed to its greater accessibility of hydroxyl groups and lower degree of processing impurities compared with gauze and cotton, which contain residual waxes and finishing agents that partially hinder reagent diffusion.

Another significant spectral feature is observed at 1600-1635 cm^{-1}, corresponding to asymmetric stretching vibrations of carboxylate anions (-COO^-). The emergence of this peak in all oxidized samples indicates partial ionization of the newly formed carboxyl groups and the presence of cellulose carboxylate salts. The relative increase in its intensity compared with the band at 1730 cm^{-1} suggests that both neutral -COOH and ionic -COO^- forms coexist in the oxidized matrix.

In the fingerprint region, characteristic bands at 1420 cm^{-1} and 1375 cm^{-1}, attributed to CH_2 scissoring and C-H bending vibrations, remain visible in all samples, implying that the primary skeletal structure of the glucopyranose units is preserved. Similarly, the absorption at 1030-1050 cm^{-1}, related to C-O-C stretching of ether linkages and glycosidic bonds, confirms that the β-1,4-linked polysaccharide backbone remains intact despite partial oxidation [45]. The presence of a distinct band near 890 cm^{-1} assigned to β-glycosidic linkages further supports the retention of the cellulose network and indicates that oxidative cleavage did not result in complete depolymerization.

Overall, the FT-IR spectra collectively demonstrate that oxidation with NaClO effectively introduces carboxyl and carbonyl functionalities into the cellulose structure while maintaining the β-1,4-linked polysaccharide skeleton. The transformation primarily occurs at the C6 hydroxyl positions of the glucose units, leading to enhanced hydrophilicity and increased surface charge, which directly contribute to the observed improvement in swelling capacity and hemostatic behavior of the oxidized cellulose materials.

The swelling properties of pristine cellulose, woven gauze, and medical cotton, as well as the corresponding oxidized samples obtained through NaClO-mediated oxidation, were investigated. The results are summarized in Figure 2 and Table S1.



A. CC samples; **B.** WG samples; **C.** MC samples; **A1.** OC samples obtained from CC; **B1.** OC samples obtained from WG; **C1.** OC samples obtained from MC.

Figure 2. Swelling properties of mono-carboxylate cellulose samples obtained by oxidizing CC, WG, and MC using NaClO solution.

As shown in Figure 2, both the initial of the cellulose-based materials and the oxidation treatment significantly influenced the water-uptake behavior of the samples. According results of investigation untreated samples of CC showed the highest swelling capacity, reaching 130±1.7% after 20 min, whereas WG and MC exhibited lower equilibrium values of 111±2.2% and 100±3.5%, respectively (Figure 2, *A*-*C* and Table S1). These differences can reasonably be attributed to variations in fiber organization, structural compactness, and the presence of residual noncellulosic constituents or processing-induced heterogeneities, all of which may restrict water diffusion into the cellulosic network.

The OC sample derived from CC exhibited the highest swelling capacity, reaching a maximum of 380±3.3% at 20 min, while the corresponding values for oxidized WG and oxidized MC were 300±3.0% and 250±2.5%, respectively (Figure 2, *A1-C1* and Table S1). In comparison with the initial materials at the same immersion time, this corresponds to an approximately 2.9-fold increase for CC, a 2.7-fold increase for WG, and a 2.5-fold increase for MC. Such a pronounced enhancement indicates that oxidation promoted a substantial increase in the affinity of the cellulose matrix toward water. The results presented in Figure 2 above are provided in Table S1.

The improved swelling behavior of the oxidized samples can be explained by chemical and structural modifications induced by NaClO treatment. Oxidation is expected to introduce additional oxygen-containing functional groups, particularly carbonyl- and carboxyl- containing moieties, into the cellulose structure. The formation of these polar groups increases the interaction of the polymer matrix with water molecules and, at the same time, reduces the strength of intermolecular hydrogen bonding between adjacent cellulose chains [48]. As a result, the supramolecular structure becomes less compact, facilitating water penetration into the interfibrillar and amorphous regions. This structural loosening is consistent with the much higher swelling values recorded for the oxidized materials.

Another notable feature is that all oxidized samples reached their maximum swelling degree at approximately 20 min, after which a slight decline was observed. For example, the swelling degree of oxidized CC decreased from 380±3.3% at 20 min to 325±2.8% at 30 min, while the corresponding values for oxidized WG and oxidized MC decreased from 300±3.0% to 255±3.3% and from 250±2.5% to 215±2.5%, respectively (Table S1). This tendency may be associated with partial relaxation or rearrangement of the swollen oxidized network, leading to the release of loosely bound water [49]. Nevertheless, despite this slight post-maximum decrease, the oxidized samples consistently retained much higher swelling capacities than their untreated counterparts, demonstrating the persistent effect of oxidation on water-retention performance.

Overall, the obtained results confirm that NaClO oxidation is an efficient route for improving the swelling characteristics of cellulose-based materials. From a comparative standpoint, the swelling performance of the studied samples followed the order OC from CC > OC from WG > OC from MC > CC > WG > MC. This trend indicates that both the chemical modification and the intrinsic structural features of the precursor material govern the final hydration behavior.

When cellulose is first oxidized till mono-carboxylate cellulose with NaClO (Figure 3, *First stage*) and subsequently re-oxidized with $NaIO_4$, oxidizes the vicinal diols in the cellulose chain to aldehyde groups. In this process, the hydroxyl groups at the C2-C3 carbon atoms cleave the C-C bond, resulting in the formation of dialdehyde cellulose (DAC). This modification enhances the reactivity and multifunctional properties of cellulose (Figure 3, *Second stage*).

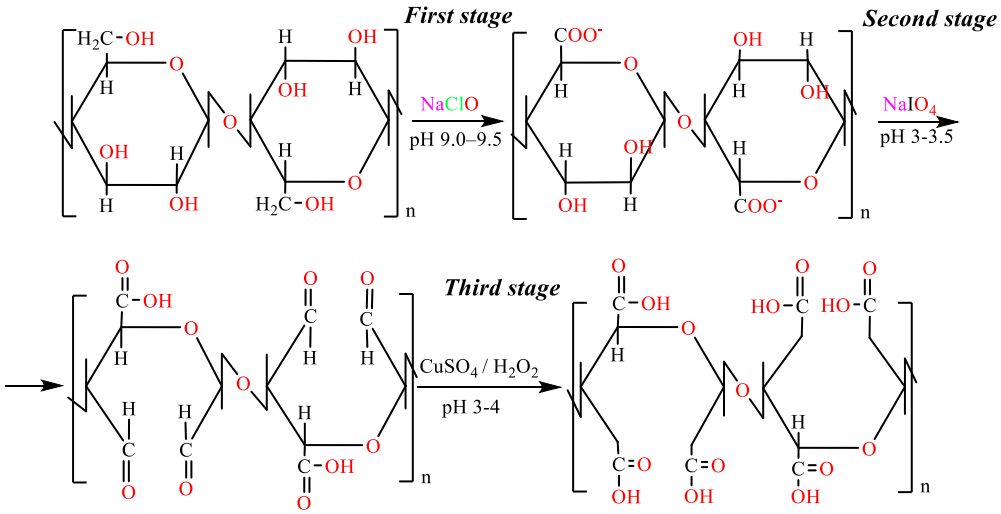


Figure 3. Schematic representation of the three-stage oxidation of cellulose using NaClO, $NaIO_4$, and H_2O_2/$CuSO_4$ to produce highly functionalized tricarboxylated cellulose.

The obtained oxycellulose sample was further oxidized with $NaIO_4$ (10-25 min, 35 °C, 2.5 % concentration), resulting in the cleavage of the C2-C3 vicinal diol and the formation of 2,3-dialdehyde

cellulose. The aldehyde group content was subsequently determined. The primary purpose of re-oxidizing oxycellulose (OC) samples, obtained through the initial oxidation of cellulose with 14 g/L NaClO, with $NaIO_4$ was to convert the vicinal diol groups located at the C2 and C3 carbon atoms into aldehyde groups (Figure 3, *Second stage*). The results are presented in Table 2.

Table 2

Oxidation of monocarboxylated cellulose with $NaIO_4$ for the synthesis of dialdehyde cellulose

Samples	C($NaIO_4$), %	pH	Reaction duration, h	T, °C	Content of aldehyde group (-CHO), mmol/g	Yield, %
OC sample obtained from CC	2.5	3.5	10	35	4.8±0.048	72±2.88
			15		5.7±0.057	61±2.44
			20		**7.2±0.072**	**55±2.21**
			25		7.4±0.074	48±1.92
OC sample obtained from WG	2.5	3.5	10	35	3.7±0.037	66±2.64
			15		4.9±0.049	58±2.32
			20		**6.2±0.062**	**56±2.24**
			25		6.4±0.064	43±1.76
OC sample obtained from MC	2.5	3.5	10	35	3.2±0.032	75±3.01
			15		4.3±0.043	66±2.64
			20		**5.0±0.051**	**56±2.22**
			25		5.3±0.053	47±1.88

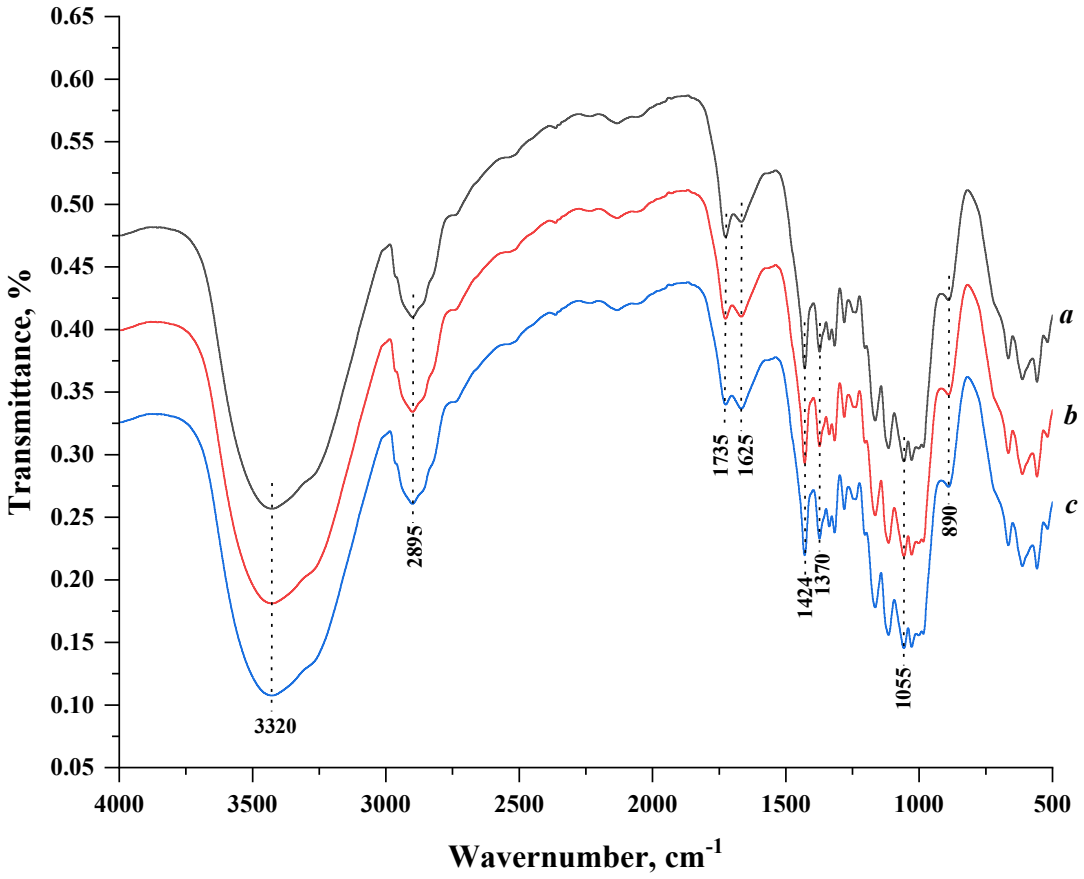
As shown in Table 2, the conversion of oxycellulose (OC) to dialdehyde cellulose was achieved by oxidation with a 2.5 % $NaIO_4$ solution under controlled pH conditions at 35 °C for reaction times ranging from 10 to 25 min. At 35 °C, $NaIO_4$ demonstrates high oxidative activity, ensuring efficient selective oxidation. However, further increases in temperature accelerate the decomposition of $NaIO_4$, thereby reducing the overall efficiency of the oxidation process.

When the reaction temperature exceeds 35 °C, the activity of periodate decreases, resulting in a reduced material yield. The oxidation process with $NaIO_4$ was carried out in an acidic medium at a pH of around 3.5, under which conditions $NaIO_4$ exhibits maximum activity, selectively converting the C2-C3 diol groups in the cellulose structure into aldehyde groups [50].

Considering the above, the reaction conditions were determined as pH 3.5, a reaction duration of 20 minutes, and a temperature of 35 °C. Under these conditions, the aldehyde group content was found to be 7.2 ±0.072 mmol/g in the DAC obtained from CC, 6.2±0.062 mmol/g in the DAC obtained from WG, and 5.0±0.051 mmol/g in the DAC obtained from MC. These values enhance the activity of dialdehyde cellulose and increase its potential for further modifications. The yield of the process was found to be 55 %, 56 %, and 56 %, respectively. The yield was found to depend on the reaction conditions. When the pH, temperature, or reaction time exceeded the reaction conditions range, a significant decrease in yield was observed.

The FT-IR spectra of the dialdehyde cellulose samples obtained by re-oxidizing oxycellulose (OC) with sodium periodate ($NaIO_4$) are presented in Figure 4.

The FT-IR spectra shown in Figure 4 clearly reveal the structural changes occurring in CC, WG, and MC during the secondary oxidation of the NaClO-treated samples with $NaIO_4$, leading to the formation of dialdehyde cellulose. This oxidation pathway selectively cleaves the vicinal hydroxyl groups at the C2 and C3 carbon atoms of the anhydroglucose units, forming DAC. The spectral profiles of the samples thus reflect the successful conversion of hydroxyl functionalities into aldehyde and carboxyl groups, as well as the partial rearrangement of the polysaccharide backbone.



a. Dialdehyde cellulose obtained by the oxidation of CC; **b.** Dialdehyde cellulose obtained by the oxidation of WG; **c.** Dialdehyde cellulose obtained by the oxidation of MC.

Figure 4. Results of FT-IR spectroscopic analysis of dialdehyde cellulose samples.

In the spectrum of unmodified cotton cellulose, a broad and intense absorption band at 3340-3400 cm^{-1} corresponds to O-H stretching vibrations associated with inter- and intramolecular hydrogen bonding (Figure 4, *a*). After $NaIO_4$ oxidation of CC till aldehyde cellulose, the intensity of this band markedly decreases and shifts slightly toward lower wavenumbers (~3320 cm^{-1}), suggesting the consumption of a portion of the hydroxyl groups during oxidation and the consequent reduction of hydrogen-bond density (Figure 4, *b*). This spectral change is accompanied by a mild increase in baseline absorbance, reflecting enhanced amorphousness and increased molecular disorder within the cellulose matrix.

The most notable difference between the native and oxidized samples is the appearance of a strong new band at 1730-1740 cm^{-1}, assigned to the C=O stretching vibration of aldehyde groups (-CHO) and, to a lesser extent, carboxyl groups (-COOH). This band is absent in pristine cellulose but becomes prominent in all $NaIO_4$-oxidized spectra, confirming the successful formation of dialdehyde cellulose (Figure 4, *b*-*c*). The relative intensity of the 1730 cm^{-1} band follows the order CC > WG > MC, indicating that pure cellulose undergoes the highest degree of oxidation. This trend is consistent with the experimentally determined aldehyde group contents of 7.2±0.072, 6.2±0.062, and 5.0±0.051 mmol/g, respectively (Table 2). The higher reactivity of pure cellulose is attributed to its greater accessibility of secondary hydroxyl groups and lower structural compactness compared with gauze and cotton, whose denser fiber morphology restricts periodate penetration.

A distinct absorption peak near 1625 cm^{-1} is observed in all oxidized spectra, which can be attributed to asymmetric stretching vibrations of ionized carboxylate groups ($-COO^-$). This suggests that partial over-oxidation of aldehyde groups to carboxylic acids occurred during the reaction or subsequent drying. The coexistence of carbonyl and carboxylate functionalities enhances the overall polarity of the oxidized matrix, explaining the improved hydrophilicity and sorption behavior observed in subsequent experiments.

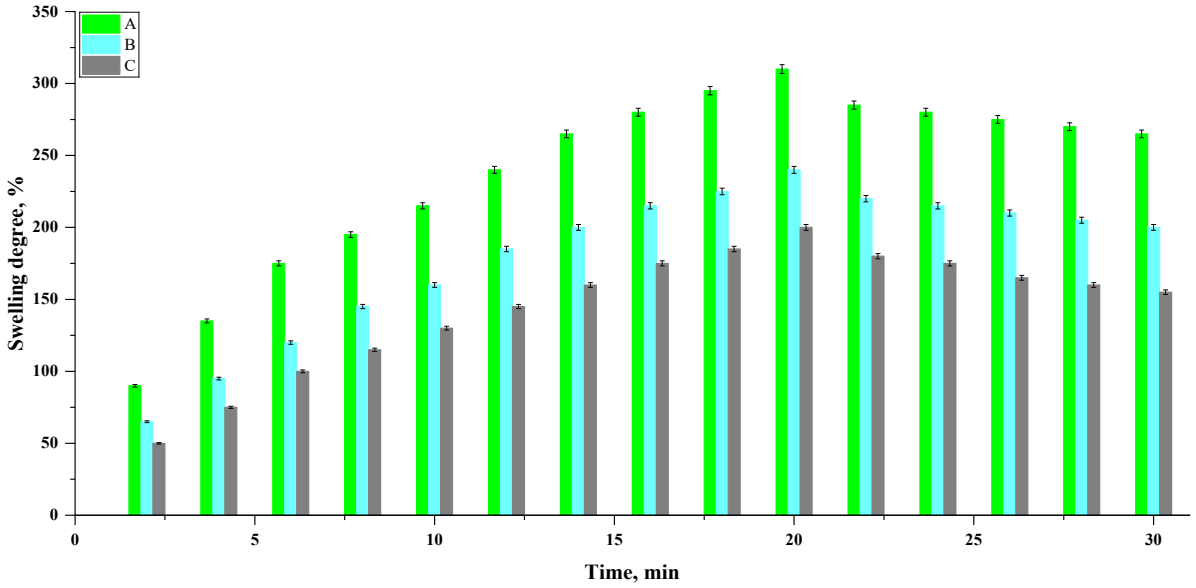
In the region of 1130-1150 cm^{-1}, a moderate-intensity band associated with C-O stretching of hemiacetal linkages is detected. The emergence of this peak indicates the possible intramolecular reaction

between newly formed aldehyde and neighboring hydroxyl groups, yielding hemiacetal structures and crosslinked domains within the cellulose network. These spectral changes imply a partial reconstruction of the polymer matrix toward a more compact configuration, consistent with literature reports [50] on DAC formation.

The bands at 1050 cm^{-1} (C-O-C stretching of glycosidic bonds) and 890 cm^{-1} (β-glycosidic linkages) remain visible, confirming that despite oxidation-induced cleavage at C2-C3, the fundamental β-1,4-linked polysaccharide framework is largely preserved. However, a slight decrease in their intensity indicates partial chain scission and local disruption of crystallinity.

A comparative evaluation among the three oxidized materials reveals that the DAC obtained from CC exhibits the strongest C=O absorption at 1735 cm^{-1} and the most pronounced decrease in the O-H band, demonstrating the highest oxidation efficiency (Figure 4, *b*). The DAC obtained from WG shows intermediate characteristics, where both aldehyde and carboxylate peaks appear with moderate intensity, suggesting partial oxidation limited by lower surface accessibility (Figure 4, *c*). In contrast, the DAC derived from MC exhibits a broader hydroxyl stretching band and a less intense carbonyl signal, which may be attributed to its higher crystallinity and residual finishing agents that limit the penetration of the $NaIO_4$ solution into the interior regions of the fibers (Figures 4, *c*).

Overall, the FT-IR spectra of $NaIO_4$-oxidized samples of DAC confirm the selective cleavage of vicinal diols (C2-C3) in cellulose and the formation of dialdehyde and carboxyl functionalities while maintaining the β-1,4-glucopyranose backbone . This transformation increases the reactivity of the cellulose matrix, enhances its hydrophilicity, and provides abundant reactive aldehyde sites suitable for further functionalization to tricarboxycellulose during subsequent oxidation with hydrogen peroxide (Figure 5 and Table S2).



A. DAC samples obtained from CC; **B.** DAC samples obtained from WG; **C.** DAC samples obtained from MC.
Figure 5. Swelling properties of DAC samples obtained by $NaJO_4$.

A decrease in the swelling degree was observed in all samples oxidized with periodate compared with those oxidized with NaClO. Specifically, the swelling degree of the DAC samples obtained from OC, WG, and MC decreased by 17 %, 15 %, and up to 20 %, respectively, following periodate oxidation. This reduction can be attributed to the formation of carbonyl groups in the sample structure during periodate oxidation, which alters the interactions between the samples and water. The introduction of carbonyl groups into the macromolecular structure may modify the hydrophilic–hydrophobic balance and reduce the accessibility of water to the polymer chains, thereby contributing to a substantial decrease in the swelling degree.

In the next stage, reactions were carried out to obtain tricarboxycellulose through the stepwise oxidation of CC, WG, and MC using hydrogen peroxide (Figure 3, *Third stage*). The resulting products were characterized by a high content of carboxyl groups, as well as enhanced hydrophilic and reactive properties. The

obtained DAC sample was oxidized (2-3 h, 70-80°C, 6-8% concentration) to oxidize the C6 and C2-C3 carbon atoms, yielding tricarboxycellulose. The results are presented in Table 3.

As shown in the Tables 3 of the obtained results, an increase in the concentration of the oxidizing agent and the reaction time during the oxidation process led to a decrease in product yield.

Table 3

The variation in the content of carboxyl groups depends on the duration of the modification process and the concentration of the oxidizing agent *(pH reaction 3-4)*

No.	Samples	$C(H_2O_2)$, %	Time, hour	Content of carboxyl groups (-COOH), mmol/g	Yield, %
1	DAC obtained from CC	6	2	8.53±0.09	47±0.61
2	DAC obtained from WG	6	2	7.13±0.08	50±0.75
3	DAC obtained from MC	6	2	6.35±0.07	52±0.92
4	DAC obtained from CC	8	3	11.95±0.12	35±0.15
5	DAC obtained from WG	8	3	10.55±0.11	38±0.32
6	DAC obtained from MC	8	3	9.40±0.10	41±0.45

Meanwhile, the content of carboxyl groups in the samples increased, reaching 9.40±0.10 mmol/g in tricarboxycellulose obtained from oxidized MC (Table 3, *No. 6*), 10.55±0.11 mmol/g in tricarboxycellulose obtained from oxidized WG (Table 3, *No. 5*), and up to 11.95±0.12 mmol/g in tricarboxycellulose obtained from oxidized CC (Table 3, *No. 4*). This demonstrates the possibility of obtaining tricarboxycellulose compounds highly enriched with carboxyl groups through the oxidation of the C6, C2, and C3 elementary units. The yield was found to decrease by up to 35±0.15 %. This indicates that the observed material loss resulted from the cleavage of the main polymer chains, fragmentation of the crystalline regions, and the formation of amorphous domains during the oxidation reactions. Therefore, although the yield was relatively low, the high extent of modification during the process was confirmed.

The FT-IR spectra of tricarboxycelluloses prepared from oxidized of CC, WG, and MC using H_2O_2 are presented in Figure 6.

The FT-IR spectra shown in Figure 6 provide clear evidence of the multistage oxidation of CC, WG, and MC using NaClO, $NaIO_4$, and H_2O_2. The progressive transformation of hydroxyl groups into carbonyl and carboxyl functionalities, accompanied by partial depolymerization and amorphization, is reflected in significant spectral changes compared with both the pristine and DAC samples.

In all tricarboxycellulose samples, a broad absorption band located in the range of 3300-3400 cm^{-1} corresponds to O-H stretching vibrations of hydroxyl groups linked through intra- and intermolecular hydrogen bonds. The intensity of this band is notably reduced relative to the initial cellulose and DAC samples, confirming that a substantial fraction of hydroxyl groups has been converted into carboxyl groups (-COOH). Furthermore, a slight shift of this band toward lower wavenumbers (≈ 3320 cm^{-1}) suggests stronger hydrogen bonding between remaining hydroxyl and newly formed carboxyl functionalities, which enhances the hydrophilic and ion-exchange properties of the material.

The most diagnostic spectral feature of tricarboxycellulose appears as a strong and sharp absorption band in the region of 1725-1735 cm^{-1}, assigned to the C=O stretching vibrations of carboxylic acid groups [51]. This peak exhibits much higher intensity than in the $NaIO_4$-oxidized samples (Figure 6), confirming the complete oxidation of both primary (C6) and secondary (C2, C3) hydroxyl groups into carboxyl moieties. The band intensity follows the order CC > WG > MC, consistent with the experimentally determined carboxyl contents 11.95±0.12 mmol/g, 10.55±0.11 mmol/g, and 9.40±0.10 mmol/g, respectively (Figure 6, *a-c*). This correlation demonstrates that pure cellulose undergoes the most extensive oxidation due to its greater accessibility of reactive sites and lower fiber compactness compared with woven and medical cotton matrices.

Another important feature is the pronounced band at 1605-1620 cm^{-1}, corresponding to the asymmetric stretching of carboxylate anions ($-COO^-$). The coexistence of this band with the C=O absorption at 1730 cm^{-1} indicates that part of the carboxylic groups are ionized, forming sodium or protonated salts during neutralization and drying. This dual presence of -COOH and $-COO^-$ functionalities enhances the water-binding and swelling behavior of the tricarboxycellulose samples, explaining their exceptionally high sorption capacities [52].

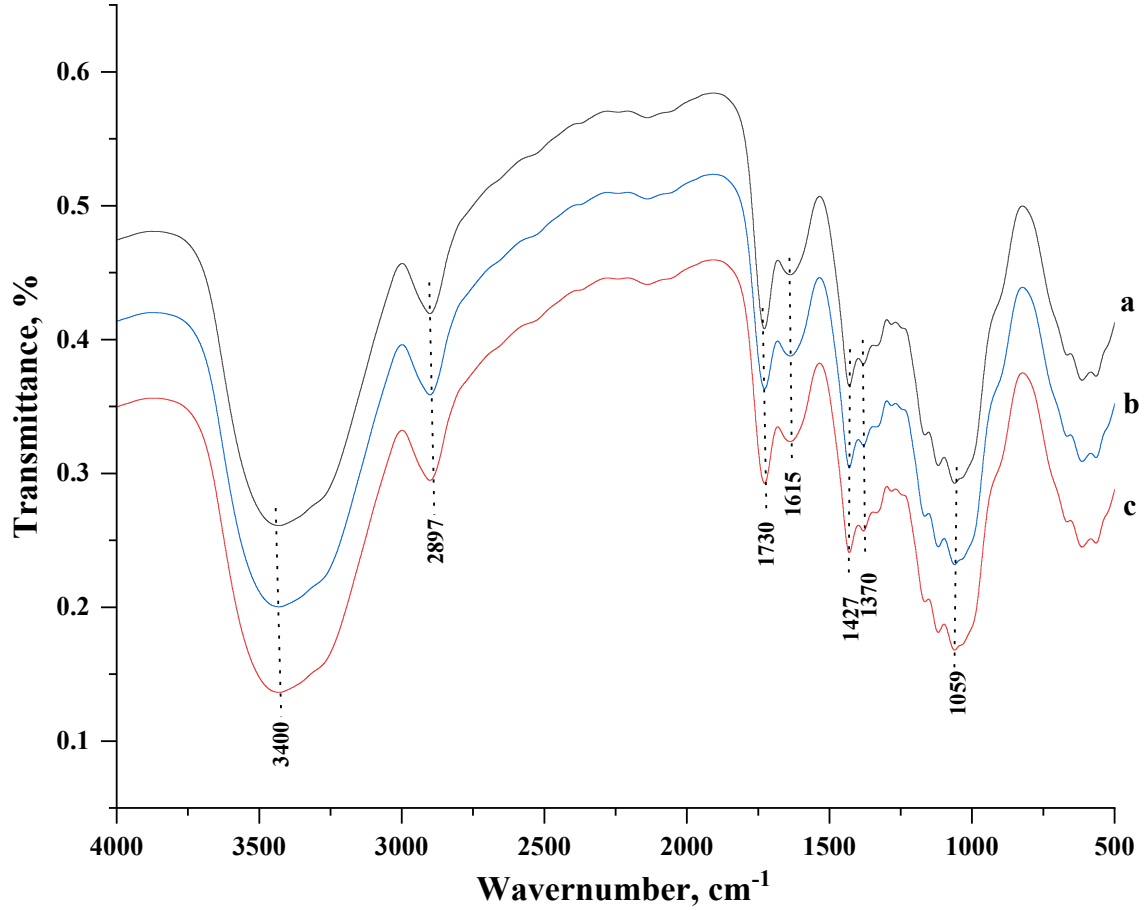


Figure 6. FT-IR spectra of tricarboxycellulose obtained from oxidized CC *(a)*, WG *(b)*, and MC *(c)*.

The spectral region around 1420 cm^{-1} (CH_2 bending) and 1370 cm^{-1} (C-H deformation) remains clearly visible in all samples, confirming that the main polysaccharide skeleton is preserved despite heavy oxidation. Similarly, the bands at 1030-1060 cm^{-1}, corresponding to C-O-C stretching of glycosidic linkages, and the 890 cm^{-1} band assigned to β-1,4-glycosidic bonds, are retained. This persistence indicates that oxidation proceeds mainly through substitution and cleavage of side groups rather than total chain destruction. Consequently, the β-1,4-glucopyranose backbone remains intact, ensuring the mechanical integrity of the oxidized fibers.

The comparative analysis among the three tricarboxycellulose variants reveals several key differences. The cellulose-derived tricarboxycellulose exhibits the most intense C=O absorption and the lowest O-H band intensity, confirming the highest oxidation efficiency and degree of functionalization. The woven gauze sample shows moderate C=O and COO^- intensities, suggesting effective yet incomplete oxidation due to the denser fiber arrangement that restricts reagent diffusion. The medical cotton sample, on the other hand, presents broader and less intense carbonyl peaks, which can be attributed to its higher crystallinity and presence of residual surface treatments that hinder reagent accessibility.

Notably, the simultaneous increase in the intensity of both 1730 cm^{-1} (-COOH) and 1615 cm^{-1} ($-COO^-$) bands signifies that hydrogen peroxide oxidation not only converts remaining aldehyde groups from the DAC stage into carboxyl functionalities but also induces partial ionization. This dual modification substantially increases the polarity and water affinity of the material. The resulting molecular architecture thus contains multiple hydrophilic sites capable of strong hydrogen bonding with water molecules, accounting for the enhanced sorption and hemostatic performance observed experimentally.

Overall, the FT-IR spectral results of Figure 6 confirm that the sequential oxidation of cellulose using $NaClO \rightarrow NaIO_4 \rightarrow H_2O_2$ successfully yields tricarboxycellulose enriched with carboxyl and carboxylate groups while preserving the core β-1,4-linked polysaccharide framework. The stepwise conversion of hydroxyl and aldehyde groups into -COOH functionalities fundamentally transforms the physicochemical

profile of cellulose, resulting in a biopolymer with superior hydrophilicity, ion-exchange capacity, and biocompatibility essential characteristics for its application as an efficient biodegradable hemostatic material.

The swelling properties of cellulose-based materials depend on their chemical composition, structural amorphousness, and degree of modification [53]. Oxidative functionalization of cellulose, particularly through enrichment with carboxyl groups, enhances its interaction with water. The swelling properties of tricarboxycelluloses obtained from CC, WG, and MC were investigated, and the corresponding results are presented in Figure 7 and Table S3.

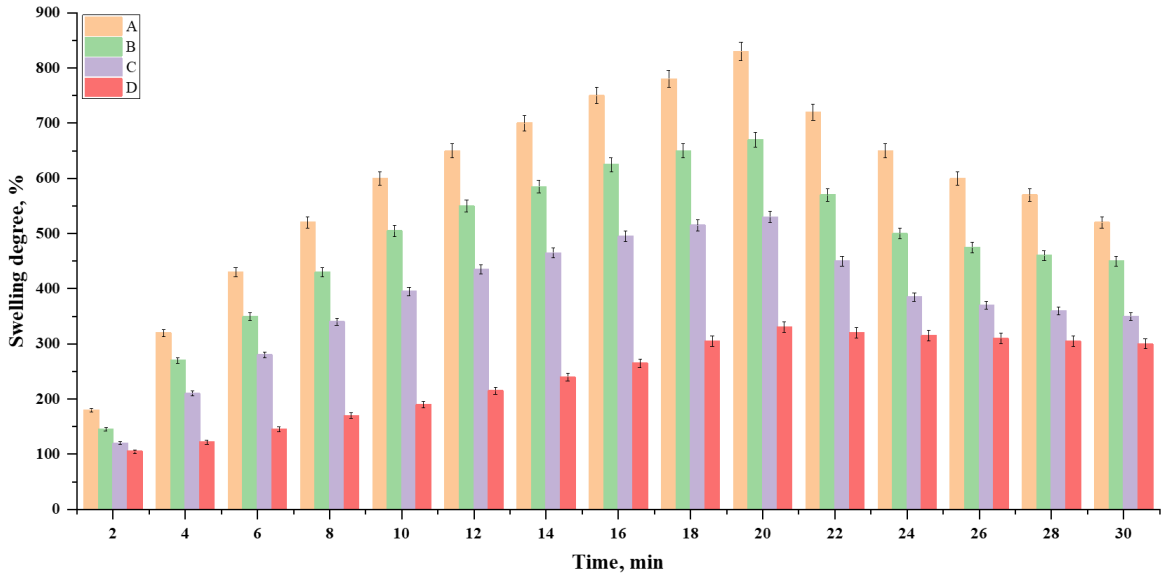


Figure 7. Effect of time on the swelling degree of tricarboxycelluloses derived from CC (A), WG (B), MC (C) and SURGICEL® Powder (D).

Among the investigated samples, tricarboxycellulose derived from cotton cellulose (TCC–CC) exhibited the highest swelling capacity. Its swelling degree increased from 180±3.6% at 2 min to 830±16.6% at 20 min, followed by a decrease to 550±10.4% at 30 min (Figure 7A).

A similar trend was observed for tricarboxycellulose derived from woven gauze (TCC–WG), with the swelling degree increasing from 145±2.9% at 2 min to 670±13.4% at 20 min and subsequently decreasing to 450±9.0% at 30 min (Figure 7B).

Tricarboxycellulose obtained from medical cotton (TCC-MC) exhibited a lower swelling capacity than the other synthesized samples. Its swelling degree increased from 120±2.4% at 2 min to 530±10.6% at 20 min, followed by a decline to 351±7.0% at 30 min (Figure 7C).

For comparison, the commercial hemostatic material SURGICEL® Powder exhibited a swelling degree of 105±3.15% at 2 min, which increased to a maximum of 330±9.90% at 20 min before decreasing to 300±9.01% at 30 min (Figure 7D). These results demonstrate that SURGICEL® Powder exhibited a lower swelling capacity than all three synthesized tricarboxycellulose samples under the investigated experimental conditions.

Accordingly, the maximum swelling capacities of the investigated materials followed the order: TCC-CC > TCC-WG > TCC-MC > SURGICEL® Powder.

The obtained results indicate that the tricarboxycellulose materials synthesized through the sequential three-step oxidation process exhibited higher swelling capacities than the commercial SURGICEL® Powder hemostatic material. These differences may be associated with variations in carboxyl functional group content, hydrophilicity, and structural and morphological characteristics of the investigated materials. The initial increase in swelling degree may be attributed to the gradual diffusion of water into the polymer matrix and the hydration of hydrophilic functional groups, particularly carboxyl groups introduced during oxidation. These groups promote stronger interaction with water and facilitate expansion of the cellulose network. The higher swelling values exhibited by the cotton cellulose-derived sample may be associated with the increased accessibility of hydrophilic functional groups and the development of a less ordered supramolecular structure. Such structural changes facilitate the diffusion of water molecules into the cellulose matrix and enhance water retention, resulting in improved swelling performance [54].

Overall, the results demonstrate that both the precursor type and the swelling duration play a decisive role in determining the swelling behavior of tricarboxycelluloses. From a practical viewpoint, tricarboxycellulose derived from cotton cellulose appears to be the most promising sample for applications requiring high water uptake. The significant increase in swelling capacity after multistage oxidation can be explained as follows [55]:

NaClO oxidation primarily converts a portion of the C6 hydroxyl groups into carboxyl groups, increasing surface polarity;

$NaIO_4$ oxidation selectively cleaves vicinal diols at C2-C3 positions, forming aldehyde groups and disrupting crystalline domains. This partial cleavage introduces amorphous regions and exposes internal hydroxyl sites, facilitating subsequent reactions;

H_2O_2 oxidation completes the transformation by converting the remaining aldehydes into additional carboxyl groups. The resulting tricarboxycellulose thus contains multiple -COOH and $-COO^-$ functionalities distributed along the polymer backbone. These groups act as active hydrophilic centers capable of forming hydrogen bonds with water molecules and electrostatically binding cations in physiological media;

From a structural standpoint, the enhanced swelling of tricarboxycellulose arises from two synergistic effects [56]: (a) chemical modification, which increases the number of hydrophilic sites per macromolecule, and (b) physical restructuring, which creates a more open, porous, and amorphous matrix that allows easier diffusion of water. The oxidation-induced cleavage of hydrogen bonds and partial disruption of crystalline regions enlarge the specific surface area, while the introduction of negatively charged carboxylate groups enhances water affinity through ion-dipole interactions.

In addition, the swelling behavior illustrated in Figure 7 confirms that tricarboxycellulose obtained via the $NaClO \rightarrow NaIO_4 \rightarrow H_2O_2$ oxidation route possesses markedly enhanced hydrophilicity and liquid absorption capacity compared with its precursor materials. The observed trend cellulose > woven gauze > medical cotton is fully consistent with both chemical and structural analyses. The combination of high carboxyl group content, expanded amorphous regions, and increased surface charge endows tricarboxycellulose with excellent swelling, ion-exchange, and hemostatic properties, making it a promising candidate for use as an efficient biodegradable wound-dressing and hemostatic agent.

The hemostatic properties of tricarboxycellulose samples synthesized via the stepwise oxidation of CC, WG, and MC using $NaClO \rightarrow NaIO_4 \rightarrow H_2O_2$ were investigated, and the results are presented in Table 4.

As shown in Table 4, the hemostatic performance of the tricarboxycellulose-based samples was strongly affected by the carboxyl group content and molecular mass. Among the tested samples tricarboxycellulose obtained from cellulose exhibited the highest carboxyl group content of 11.95±0.12 mmol/g. This sample demonstrated the shortest bleeding time, 69±3.24 s, and the lowest blood clotting index 55.6±0.15%, indicating the most effective hemostatic activity (Table 4, *No.1*).

The tricarboxycellulose obtained from woven gauze also showed relatively good performance, with a carboxyl group content of 10.55±0.11 mmol/g, bleeding time of 78±4.14 s, and blood clotting index of 62.9±0.32 % (Table 4, *No. 2*). However, its hemostatic efficiency was lower than that of the sample *No. 1*. This difference may be associated with its lower degree of oxidation and reduced availability of carboxyl groups.

Table 4

Results of hemostatic properties of the tricarboxycellulose samples

No.	Samples of tricarboxy cellulose	Content of carboxyl groups (-COOH), mmol/g	Bleeding time, s	Blood clotting index, %
1	Obtained from CC	11.95±0.12	69±3.24	55.6±0.15
2	Obtained from WG	10.55±0.11	78±4.14	62.9±0.32
3	Obtained from MC	9.40±0.10	111±4.46	86.2±0.45
4	SURGICEL® Powder	5.35±0.08	124±4.62	89.5±0.47

The tricarboxycellulose obtained from medical cotton showed a further decrease in hemostatic efficiency. Its carboxyl group content was 9.40±0.10 mmol/g, and the bleeding time increased to 111 ± 4.46 s, while the blood clotting index reached 86.2±0.45 % (Table 4, *No. 3*). These results suggest that a lower amount of carboxyl groups reduces the ability of the material to accelerate blood coagulation.

The commercial SURGICEL® Powder sample showed the lowest carboxyl group content, 5.35±0.08 mmol/g, and the longest bleeding time, 124±4.62 s, with the highest blood clotting index of 89.5±0.47 % (Table 4, *No. 4*). In comparison with the prepared tricarboxycellulose samples, this indicates weaker hemostatic performance under the same experimental conditions.

Overall, the results show that increasing the carboxyl group content improves the hemostatic activity of tricarboxycellulose materials. The tricarboxycellulose obtained from different cellulose materials demonstrated the best balance of high carboxyl group content, rapid bleeding control, and low blood clotting index. Therefore, this material can be considered the most promising candidate for the development of an effective powdered hemostatic agent.

Conclusions

In this study, highly functionalized tricarboxycellulose materials were successfully synthesized from CC, WG, and MC through a sequential three-step oxidation strategy employing sodium hypochlorite (NaClO), sodium periodate ($NaIO_4$), and hydrogen peroxide (H_2O_2). The proposed oxidation pathway enabled the controlled conversion of cellulose hydroxyl groups into aldehyde and subsequently carboxyl functionalities, resulting in materials with a high density of reactive oxygen-containing groups and significantly enhanced physicochemical properties.

FT-IR spectroscopic analysis provided clear evidence of the progressive structural transformation occurring during each oxidation stage. The gradual decrease in the intensity of hydroxyl-related absorption bands, together with the appearance and strengthening of characteristic carbonyl and carboxyl absorption peaks at 1730-1740 cm^{-1} and carboxylate bands near 1615 cm^{-1}, confirmed the successful formation of tricarboxycellulose. The highest degree of oxidation was achieved for CC, WG and MC, corresponding to carboxyl group contents of 11.95±0.12 mmol/g, 10.55±0.11 mmol/g, and 9.40±0.10 mmol/g, respectively.

Tricarboxycellulose samples obtained from CC, WG and MC exhibited exceptionally high swelling capacities, reaching 830±16.6 %, 670±13.4 %, and 530±10.6 % respectively. This remarkable increase in water uptake can be attributed not only to the increased concentration of hydrophilic functional groups but also to oxidation-induced disruption of crystalline domains, partial cleavage of intermolecular hydrogen-bonding networks, and the formation of a more open and porous supramolecular architecture. The synergistic effect of chemical functionalization and structural reorganization substantially enhanced water diffusion and retention within the cellulose matrix.

Furthermore, the hemostatic investigations demonstrated a strong relationship between the degree of oxidation, swelling capacity, and blood-clotting efficiency. The tricarboxycellulose materials obtained from CC, WG and MC significantly accelerated coagulation, yielding clotting times of 69±3.24 s, 78±4.14 s, and 111±4.46 s respectively. The superior hemostatic performance is attributed to the rapid absorption of blood plasma, concentration of coagulation factors at the wound site, and enhanced interactions between negatively charged carboxylate groups and blood components, which collectively promote platelet adhesion, activation, and fibrin network formation. Notably, the cellulose-derived tricarboxycellulose outperformed the commercial hemostatic material SURGICEL® Powder, highlighting its potential as an advanced hemostatic agent.

Overall, the results demonstrate that sequential $NaClO \rightarrow NaIO_4 \rightarrow H_2O_2$ oxidation represents an efficient and versatile approach for producing tricarboxycellulose with a high carboxyl group content, excellent swelling performance, and outstanding hemostatic activity. The combination of biodegradability, biocompatibility, high liquid absorption capacity, and rapid blood-clotting ability makes these materials promising candidates for next-generation wound dressings, surgical hemostats, tissue-regeneration scaffolds, and other biomedical applications. Future studies should focus on in vivo biocompatibility assessment, degradation behavior, cytotoxicity evaluation, and clinical validation to further establish the practical applicability of tricarboxycellulose as a safe and effective biomaterial for advanced healthcare technologies.

Supporting Information

The Supporting Information is available free at https://ejc.buketov.edu.kz/ejc/article/view/818/450

Funding

This research was funded by the applied project on the topic AL-11725099248; AL-9224093921 "Development of a new original preparation based on nanostructured biopolymers with hemostatic and mucoadhesive properties for the non-surgical treatment of stomach and duodenal ulcer disease" for the years 2025-

2027 by the Innovative Development Agency under the Ministry of High Education, Science and Innovation of the Republic of Uzbekistan and fundamental program of Academy of Sciences of the Republic of Uzbekistan “Scientific foundations of the functionalization of natural biopolymers and their derivatives for the purpose of activation” for the year 2026-2027.

*Author Information**

**The authors' names are presented in the following order: First Name, Middle Name and Last Name*

Bakhriddin Zhumaevich Kholturaev - PhD in Chemistry, Junior Researcher, Laboratory of Chemistry and Technology of Cellulose and Its Derivatives, Institute of Polymer Chemistry and Physics, Academy of Sciences of the Republic of Uzbekistan, Abdulla Kadiri Street, 7-b, 100128, Tashkent, Uzbekistan; e-mail: bakhriddinjumayevich@gmail.com; https://orcid.org/0009-0004-6821-3149

Khaydar Ergashovich Yunusov *(corresponding author)* - Doctor of Technical Sciences, Professor, Laboratory of Chemistry and Technology of Cellulose and Its Derivatives, Institute of Polymer Chemistry and Physics, Academy of Sciences of the Republic of Uzbekistan, Abdulla Kadiri Street, 7-b, 100128, Tashkent, Uzbekistan; e-mail: silver4727@yahoo.com; https://orcid.org/0000-0002-4646-7859

Sherzod Abdullaevich Yuldoshov - Doctor of Chemical Sciences, Senior Researcher, Laboratory of Chemistry and Technology of Cellulose and Its Derivatives, Institute of Polymer Chemistry and Physics, Academy of Sciences of the Republic of Uzbekistan, Abdulla Kadiri Street, 7-b, 100128, Tashkent, Uzbekistan; e-mail: sherzodbek_y@mail.ru; https://orcid.org/0000-0002-5690-4426

Abdushkur Abdukhalilovich Sarymsakov - Doctor of Technical Sciences, Professor, Institute of Polymer Chemistry and Physics, Academy of Sciences of the Republic of Uzbekistan, Abdulla Kadiri Street, 7-b, 100128, Tashkent, Uzbekistan; e-mail: sarimsakov1948@mail.ru; https://orcid.org/0000-0002-1345-5288

Abdumutolib Abdupatto Ugli Atakhanov - Doctor of Technical Sciences, Professor, Director of the Institute of Polymer Chemistry and Physics, Academy of Sciences of the Republic of Uzbekistan, Abdulla Kadiri Street, 7-b, 100128, Tashkent, Uzbekistan; e-mail: a.atakhanov@yandex.ru; https://orcid.org/0000-0002-4975-3658

Ziyoviddin Zaynidinovich Xakimov - Doctor of Medical Sciences, Professor, Key Laboratory of Pharmaco-Toxicological Research, Tashkent Medical Academy, Tashkent, Uzbekistan; e-mail: khakimov-ziyaviddin@gmail.com; https://orcid.org/0009-0002-0046-5724

Somia Yassin Hussain Abdalkarim - PhD in Textile Engineering, Research Associate Professor, College of Textile Science and Engineering (International Institute of Silk), Zhejiang Sci-Tech University, No. 928, Second Avenue, Xiasha Higher Education Zone, Hangzhou, Zhejiang, China; e-mail: somia@zstu.edu.cn; https://orcid.org/0000-0002-4987-7730

Houyong Yu - PhD, Professor, College of Textile Science and Engineering (International Institute of Silk), Zhejiang Sci-Tech University, Hangzhou, 310018, China; e-mail: phdyu@zstu.edu.cn; https://orcid.org/0000-0002-6543-5924

Guohua Jiang - PhD, Professor, School of Materials Science and Engineering, Zhejiang Sci-Tech University, Hangzhou, 310018, China; e-mail: ghjiang_cn@zstu.edu.cn; https://orcid.org/0000-0003-3666-8216

Li-Na Niu - PhD, Professor, Department of Prosthodontics, School of Stomatology, The Fourth Military Medical University (Air Force Medical University), Xi'an, 710032, China; e-mail: niulina831013@126.com; https://orcid.org/0000-0002-6653-0819

Author Contributions

The manuscript was written through contributions of all authors. All authors have given approval to the final version of the manuscript. **Bakhriddin Zh. Kholturaev -** Investigation, Writing-Original Draft & Methodology; **Khaydar E. Yunusov -** Writing – review & editing, Methodology, Project administration, Conceptualization; **Sherzod A. Yuldoshov -** Writing – review & editing; **Abdushkur A. Sarymsakov -** Supervision & Visualization: **Abdumutolib A. Atakhanov -** Review & editing; **Ziyoviddin Z. Xakimov -** Review & editing; **Somia Yassin Hussain Abdalkarim -** Writing – Review & Editing; **Houyong Yu -** Review & Editing; **Guohua Jiang -** Writing – Original Draft, Methodology, Resources; **Li-Na Niu -** Writing – Review & Editing.

Acknowledgment

The authors express their sincere gratitude to the Physical and Physicochemical Research Laboratory of the Institute of Polymer Chemistry and Physics, Academy of Sciences of the Republic of Uzbekistan, for their valuable support in conducting the physicochemical studies. We also extend our heartfelt thanks to the research staff of the Tashkent Medical Academy for their assistance with the medical-biological analyses. Furthermore, we are deeply grateful to Zhejiang Sci-Tech University for their cooperation and technical support in carrying out the physicochemical and biomedical investigations presented in this work.

Conflict of interest

The authors declare that there is no conflict of interests regarding the publication of this article.

Declaration of AI-Assisted Language Editing

During the preparation of this manuscript, the authors used an AI-assisted tool to correct grammatical errors and improve the language, clarity, and readability of the manuscript. The tool was not used to generate scientific data, interpret experimental results, and formulate scientific conclusions. The authors carefully reviewed, edited, and verified the entire manuscript and approved its final version. The authors take full responsibility for the accuracy, integrity, and scientific content of the publication.

References

1 Grzybek, P., Dudek, G., & Van der Bruggen, B. (2024). Cellulose-based films and membranes: A comprehensive review on preparation and applications. *Chemical Engineering Journal, 495*, Article 153500. https://doi.org/10.1016/j.cej.2024.153500

2 Chen, Z., Aziz, T., Sun, H., Ullah, A., Ali, A., Cheng, L., Ullah, R., & Khan, F. U. (2023). Advances and applications of cellulose bio-composites in biodegradable materials. *Journal of Polymers and the Environment, 31*(6), 2273–2284. https://doi.org/10.1007/s10924-022-02561-8

3 Nawaz, H., He, A., Wu, Z., Wang, X., Jiang, Y., Ullah, A., Xu, F., & Xie, F. (2024). Revisiting various mechanistic approaches for cellulose dissolution in different solvent systems: A comprehensive review. International Journal of Biological Macromolecules, 273, 133012. https://doi.org/10.1016/j.ijbiomac.2024.133012

4 Li, F. H., Shen, Y. Y., Deng, Y. P., Zhang, J. C., Wang, Q. Q., Chen, H. Y., Ouyang, M., Jiang, Q. W., Wang, G. W., & Zhuang, L. H. (2023). Experimental and theoretical studies on dissolution and regeneration of microcrystalline cellulose with dihydroxyl ionic liquids. *Journal of Molecular Liquids, 389*, Article 122928. https://doi.org/10.1016/j.molliq.2023.122928

5 Acharya, S., Hu, Y., & Abidi, N. (2021). Cellulose dissolution in ionic liquid under mild conditions: Effect of hydrolysis and temperature. *Fibers, 9*(1), Article 5. https://doi.org/10.3390/fib9010005

6 Wohlert, M., Benselfelt, T., Wågberg, L., Furó, I., Berglund, L. A., & Wohlert, J. (2022). Cellulose and the role of hydrogen bonds: Not in charge of everything. *Cellulose, 29*, 1–23. https://doi.org/10.1007/s10570-021-04325-4

7 Madhushree, M., Mahesha, G. T., Venkatachalam, H., & Bhat, K. S. (2026). Green approaches to the surface modification of cellulose: Methods and mechanisms. *Journal of Composites Science, 10*(2), Article 99. https://doi.org/10.3390/jcs10020099

8 Baron, R. I., Biliuta, G., Macsim, A.-M., Dinu, M. V., & Coseri, S. (2023). Chemistry of hydroxypropyl cellulose oxidized by two selective oxidants. *Polymers, 15*(19), Article 3930. https://doi.org/10.3390/polym15193930

9 Kramar, A., Korica, M., & Kostić, M. (2024). Comparative analysis of electrokinetic properties of periodate- and TEMPO-oxidized regenerated cellulose fabric functionalized with chitosan. *Textiles, 4*(1), 57–69. https://doi.org/10.3390/textiles4010005

10 Rezaei, M., Das, R., Womack, N., Shojaeian, R., Pasha, S., Davoudi, M., Yu, S., Ilacas, G., Gersappe, D., & Hsiao, B. S. (2025). Pressure effect on nitro-oxidation process for converting cellulosic biomass into carboxylated nanocelluloses. Carbohydrate Polymer Technologies and Applications, 11, 100989. https://doi.org/10.1016/j.carpta.2025.100989

11 Baseer, R. A., Dacrory, S., El Gendy, M. A. M., Ewies, E. F., & Kamel, S. (2022). A biodegradable film based on cellulose and thiazolidine bearing UV shielding property. Scientific Reports, 12, 7887. https://doi.org/10.1038/s41598-022-11457-5

12 Duceac, I. A., Tanasa, F., & Coseri, S. (2022). Selective oxidation of cellulose—A multitask platform with significant environmental impact. *Materials, 15*(14), Article 5076. https://doi.org/10.3390/ma15145076

13 Yang, Z., Qian, J., Shan, C., Li, H., Yin, Y., & Pan, B. (2021). Toward selective oxidation of contaminants in aqueous systems. *Environmental Science & Technology, 55*(21), 14494–14514. https://doi.org/10.1021/acs.est.1c05862

14 Guo, M., Ede, J. D., Sayes, C. M., Shatkin, J. A., Stark, N., & Hsieh, Y.-L. (2024). Regioselectively carboxylated cellulose nanofibril models from dissolving pulp: C6 via TEMPO oxidation and C2,C3 via periodate–chlorite oxidation. *Nanomaterials, 14*(5), Article 479. https://doi.org/10.3390/nano14050479

15 Tang, Z., Lin, X., Yu, M., Mondal, A. K., & Wu, H. (2024). Recent advances in TEMPO-oxidized cellulose nanofibers: Oxidation mechanism, characterization, properties and applications. International Journal of Biological Macromolecules, 259, 129081. https://doi.org/10.1016/j.ijbiomac.2023.129081

16 Goyibnazarov, I. Sh., Yuldoshov, Sh. A., Sarymsakov, A. A., Yunusov, Kh. E., Yarmatov, S. S., Shukurov, A. I., Bobomurodova, M. S., & Wan, Y. (2025). Obtaining dialdehyde carboxymethylcellulose through microwave treatment. *Advances in Polymer Technology, 2025*, Article 9917563. https://doi.org/10.1155/adv/9917563

17 Brault, L., Marlin, N., Mortha, G., Boucher, J., & Lachenal, D. (2025). Periodate–chlorite oxidation for dicarboxylcellulose (DCC) production: Activation strategies for the dissolution and visualization of oxidized groups distribution. *Cellulose, 32*, 723–742. https://doi.org/10.1007/s10570-024-06312-x

18 Sun, X., & Jiang, F. (2024). Periodate oxidation-mediated nanocelluloses: Preparation, functionalization, structural design, and applications. *Carbohydrate Polymers, 341*, Article 122305. https://doi.org/10.1016/j.carbpol.2024.122305

19 Xu, Y., Xu, Y., Deng, W., Chen, H., & Xiong, J. (2023). Extracting dialdehyde cellulose nanocrystals using choline chloride/urea-based deep eutectic solvents: A comparative study in $NaIO_4$ pre-oxidation and synchronous oxidation. *International Journal of Biological Macromolecules, 246*, Article 125604. https://doi.org/10.1016/j.ijbiomac.2023.125604

20 Kadsanit, K., Sriariyanun, M., Phisalaphong, M., & Kirdponpattara, S. (2025). Tailoring dialdehyde bacterial cellulose synthesis for versatile applications. Polymers, 17(13), 1836. https://doi.org/10.3390/polym17131836

21 Simon, J., Fliri, L., Drexler, F., Bacher, M., Sapkota, J., Ristolainen, M., Hummel, M., Potthast, A., & Rosenau, T. (2023). Debugging periodate oxidation of cellulose: Why following the common protocol of quenching excess periodate with glycol is a bad idea. *Carbohydrate Polymers, 310*, Article 120691. https://doi.org/10.1016/j.carbpol.2023.120691

22 Aitbella, H., Belachemi, L., Merle, N., Zinck, P., & Kaddami, H. (2024). Schiff base functionalized cellulose: Towards strong support-cobalt nanoparticles interactions for high catalytic performances. Molecules, 29(8), 1734. https://doi.org/10.3390/molecules29081734

23 Tachai, K., Deenu, A., & Kamthai, S. (2024). Short synthesis time and characterization of dialdehyde carboxymethyl cellulose (DCMC) from high bagasse carboxymethyl cellulose (CMC_β) concentration. Journal of Natural Fibers, 21(1), 2371911. https://doi.org/10.1080/15440478.2024.2371911

24 Su, Z., Cui, L., Zhang, H., Xiao, L., Chi, B., Xu, H., Ning, L., Jia, S., & Wang, X. (2023). Robust, waterproof, and degradable cellulose-based polyimine vitrimer for plastic replacement. Chemical Engineering Journal, 471, 144501. https://doi.org/10.1016/j.cej.2023.144501

25 Simon, J., Fliri, L., Fröhlich, F., Sapkota, J., Ristolainen, M., Hummel, M., Rosenau, T., & Potthast, A. (2023). Insights into the borohydride reduction of dialdehyde cellulose: The dilemma of competing reduction and β-elimination reactions. Cellulose, 30(13), 8205–8220. https://doi.org/10.1007/s10570-023-05350-1

26 Sukhatskiy, Y., Znak, Z., Sozanskyi, M., Shepida, M., Gogate, P. R., & Tsymbaliuk, V. (2024). Activated periodates and sodium percarbonate in advanced oxidation processes of organic pollutants in aqueous media: A review. *Chemistry & Chemical Technology, 18*(2), 119–130. https://doi.org/10.23939/chcht18.02.119

27 Fernández-Santos, J., Valls, C., Cusola, O., & Roncero, M. B. (2024). Periodate oxidation of nanofibrillated cellulose films for active packaging applications. International Journal of Biological Macromolecules, 267, 131553. https://doi.org/10.1016/j.ijbiomac.2024.131553

28 Zhang, Y., Deng, W., Liu, C., Yan, F., Wu, M., Cui, Q., Willför, S., Xu, C., & Li, B. (2023). Preparation of antibacterial dialdehyde nanocellulose using $LiBr{\cdot}3H_2O$ non-dissolving pretreatment promoted periodate oxidation. ACS Sustainable Chemistry & Engineering, 11(17), 6641–6651. https://doi.org/10.1021/acssuschemeng.2c07746

29 Xie, F., Fardim, P., & Van den Mooter, G. (2022). Porous soluble dialdehyde cellulose beads: A new carrier for the formulation of poorly water-soluble drugs. International Journal of Pharmaceutics, 615, 121491. https://doi.org/10.1016/j.ijpharm.2022.121491.

30 Martinsson, A., Hasani, M., & Theliander, H. (2023). The influence of transition metal ions on the oxidation of kraft pulp using hydrogen peroxide under mildly acidic conditions. *Holzforschung, 77*(5), 318–325. https://doi.org/10.1515/hf-2022-0184

31 Rafat, A. A., Verdía Barbará, P., Ullah, A., Kontturi, E., Law, R. V., & Hallett, J. P. (2025). Efficient extraction of carboxylated nanocellulose from ionoSolv pulps with alkaline H_2O_2 assisted oxidation. Cellulose, 32(2), 853–875. https://doi.org/10.1007/s10570-024-06319-4

32 Morales-Urrea, D., López-Córdoba, A., & Contreras, E. M. (2023). Inactivation kinetics of horseradish peroxidase (HRP) by hydrogen peroxide. Scientific Reports, 13, 13363. https://doi.org/10.1038/s41598-023-39687-1

33 Xiao, J., Guo, S., Wang, D., & An, Q. (2024). Fenton-like reaction: Recent advances and new trends. Chemistry – A European Journal, 30(24), e202304337. https://doi.org/10.1002/chem.202304337

34 Li, W., Song, G., Jing, J., Ren, X., Zhang, C., Oturan, M. A., & Zhou, M. (2024). Identification and quantification of reactive species in aqueous medium during application of advanced oxidation processes: A critical review. Chemical Engineering Journal, 500, 156698. https://doi.org/10.1016/j.cej.2024.156698

35 Zhang, L., Fu, J., Gao, W., Li, Y., & Fan, X. (2024). Revealing the structural variation and degradation mechanism of cellulose during ozone oxidation treatment. Industrial Crops and Products, 219, 119101. https://doi.org/10.1016/j.indcrop.2024.119101

36 Valls, C., Cusola, O., & Roncero, M. B. (2022). Evaluating the potential of ozone in creating functional groups on cellulose. *Cellulose, 29*, 6595–6610. https://doi.org/10.1007/s10570-022-04694-4

37 Poursaitidis, E. T., Gkizis, P. L., Triandafillidi, I., & Kokotos, C. G. (2024). Organocatalytic activation of hydrogen peroxide: Towards green and sustainable oxidations. Chemical Science, 15(4), 1177–1203. https://doi.org/10.1039/D3SC05618J

38 Madhushree, M., Vairavel, P., Mahesha, G. T., & Bhat, K. S. (2025). Oxidative modifications of cellulose: Methods, mechanisms, and emerging applications. *Journal of Natural Fibers, 22*(1), Article 2497910. https://doi.org/10.1080/15440478.2025.2497910

39 Li, S., Gong, L., Chen, J., Wu, X., Liu, X., Fu, H., & Shou, Q. (2024). Fabricating the multibranch carboxyl-modified cellulose for hemorrhage control. Materials Today Bio, 24, 100878. https://doi.org/10.1016/j.mtbio.2023.100878

40 Zhang, X., Ni, H., Xu, X., Li, L., Kang, H., & Li, D. (2025). Recent advancements in the synthesis, functionalization, and utilization of cellulose nanocrystals. Resources Chemicals and Materials, 4(1), 100073. https://doi.org/10.1016/j.recm.2024.05.003

41 Støpamo, F. G., Sulaeva, I., Budischowsky, D., Rahikainen, J., Marjamaa, K., Potthast, A., Kruus, K., Eijsink, V. G. H., & Várnai, A. (2024). Oxidation of cellulose fibers using LPMOs with varying allomorphic substrate preferences, oxidative regioselectivities, and domain structures. Carbohydrate Polymers, 330, 121816. https://doi.org/10.1016/j.carbpol.2024.121816

42 Brault, L., Marlin, N., Mortha, G., Boucher, J., & Lachenal, D. (2025). About the assessment of the degree of oxidation of cellulose during periodate reaction: Comparison of different characterization techniques and their discrepancies. Carbohydrate Research, 552, 109438. https://doi.org/10.1016/j.carres.2025.109438

43 Vera-Loor, A., Rigou, P., Mortha, G., & Marlin, N. (2023). Oxidation Treatments Using Hydrogen Peroxide to Convert Paper-Grade Eucalyptus Kraft Pulp into Dissolving-Grade Pulp. Molecules, 28(23), 7927. https://doi.org/10.3390/molecules28237927

44 Wang, J., Wang, Y., Liu, Z., Shao, X., Lin, Y., Song, W., Xu, D., Gao, Y., & Han, J. (2024). Modification methods' effects on the characteristics of carboxylated cellulose fibers: Carboxyl group introduction method versus physical properties. BioResources, 19(1), 1590–1601. https://doi.org/10.15376/biores.19.1.1590-1601

45 Kholturaev, B. Zh. (2023). *Polymer-based biodegradable hemostatic agent: Preparation, structure, and properties* [Candidate of chemical sciences dissertation, Institute of Chemical Physics of the Academy of Sciences of the Republic of Uzbekistan].

46 von Schreeb, A., Sjöstrand, B., Ek, M., & Henriksson, G. (2025). Drying and hornification of swollen cellulose. Cellulose, 32, 5179–5189. https://doi.org/10.1007/s10570-024-06352-3

47 Llàcer Navarro, S., Tõlgo, M., Olsson, L., & Nypelö, T. (2023). Carboxylation of sulfated cellulose nanocrystals by family AA9 lytic polysaccharide monooxygenases. Cellulose, 30, 9331–9347. https://doi.org/10.1007/s10570-023-05440-0

48 Silvestre, G. H., Pinto, L. O., Bernardes, J. S., Miwa, R. H., & Fazzio, A. (2021). Disassembling of TEMPO-oxidized cellulose fibers: Intersheet and interchain interactions in the isolation of nanofibers and unitary chains. *Cellulose, 28*, 441–455. https://doi.org/10.1007/s10570-020-03501-z

49 Sanchez-Salvador, J. L., Xu, H., Balea, A., Blanco, A., & Negro, C. (2024). Enhancement of the production of TEMPO-mediated oxidation cellulose nanofibrils by kneading. International Journal of Biological Macromolecules, 261, 129612. https://doi.org/10.1016/j.ijbiomac.2024.129612

50 Sultana, N., Edlund, U., Guria, C., & Westman, G. (2024). Kinetics of periodate-mediated oxidation of cellulose. *Polymers, 16*(3), Article 381. https://doi.org/10.3390/polym16030381

51 Knežević, N., Milanović, J., Veličković, Z., Milošević, M., Vuksanović, M. M., Onjia, A., & Marinković, A. (2023). A closed cycle of sustainable development: Effective removal and desorption of lead and dyes using an oxidized cellulose membrane. Journal of Industrial and Engineering Chemistry, 126, 520–536. https://doi.org/10.1016/j.jiec.2023.06.041

52 Park, J., Lee, D., Hwang, K., Lee, J., Lee, T.-J., Kim, Y., Kim, J. H., Lee, J., Youe, W.-J., Chun, S.-J., & Gwon, J. (2024). Effect of catalyst and oxidant concentrations in a TEMPO oxidation system on the production of cellulose nanofibers. RSC Advances, 14(45), 32852–32862. https://doi.org/10.1039/D4RA04948A

53 El Bourakadi, K., Semlali, F.-Z., Hammi, M., & El Achaby, M. (2024). A review on natural cellulose fiber applications: Empowering industry with sustainable solutions. International Journal of Biological Macromolecules, 281, 135773. https://doi.org/10.1016/j.ijbiomac.2024.135773

54 Etale, A., Onyianta, A. J., Turner, S. R., & Eichhorn, S. J. (2023). Cellulose: A review of water interactions, applications in composites, and water treatment. *Chemical Reviews, 123*(5), 2016–2048. https://doi.org/10.1021/acs.chemrev.2c00477

55 Nypelö, T., Berke, B., Spirk, S., & Sirviö, J. A. (2021). Periodate oxidation of wood polysaccharides—Modulation of hierarchies. *Carbohydrate Polymers, 252*, Article 117105. https://doi.org/10.1016/j.carbpol.2020.117105

56 Mehandzhiyski, A. Y., Engel, E., Larsson, P. A., Lo Re, G., & Zozoulenko, I. V. (2022). Microscopic insight into the structure–processing–property relationships of core–shell structured dialcohol cellulose nanoparticles. ACS Applied Bio Materials, 5(10), 4793–4802. https://doi.org/10.1021/acsabm.2c00505